Inorg. Chem. **2008**, *47*, 3158−3165

Anion Recognition of Chloride and Bromide by a Rigid Dicobalt(II) Cryptate

Jia-Mei Chen, Xiao-Mei Zhuang, Li-Zi Yang, Long Jiang, Xiao-Long Feng, and Tong-Bu Lu*

MOE Laboratory of Bioinorganic and Synthetic Chemistry, State Key Laboratory of Optoelectronic Materials and Technologies, School of Chemistry and Chemical Engineering, Sun Yat-Sen University, Guangzhou 510275, China

Received October 31, 2007

The crystal structures of $[Co_2L(Cl)](ClO_4)_3$ (**1**), $[Co_2L(Br)](ClO_4)_3$ (**2**), $[Co_2L(OH)(OH_2)]I_3$ (**3**), and $[Co_2L^1(Cl)](ClO_4)_3$ (**4**), the density functional theory calculations, as well as the binding constants of $[Co_2L]^{4+}$ toward Cl^- and Br^- and of $[Co_2L^1]^{4+}$ toward Cl^-, are reported in this paper (L = $N[(CH_2)_2NHCH_2(C_6H_4\text{-}p)CH_2NH(CH_2)_2]_3N$, L^1 = $N[(CH_2)_2NHCH_2(C_6H_4\text{-}m)CH_2NH(CH_2)_2]_3N$). The rigid dicobalt(II) cryptate $[Co_2L]^{4+}$ shows the recognition of Cl^- and Br^- but not of F^- and I^-, because of the size matching to its rigid cavity. We also found that the relative rigid tripodal skeleton of L than that of L^1 results in the higher affinity of $[Co_2L]^{4+}$ toward Cl^-. Magnetic susceptibility measurements of **1** and **2** indicate that the two Co(II) atoms in the cryptates are antiferromagnetically coupled through the Cl^-/Br^- bridge, with $g = 2.19$, $J = -13.7$ cm^{-1} for **1**, and $g = 2.22$, $J = -17.1$ cm^{-1} for **2**.

Introduction

Molecular recognition has been defined as a process involving both binding and selection of substrate(s) by a given receptor molecule,[1] and anion recognition continues to be a major research goal for many supramolecular chemistry groups around the world,[2–4] because most of the important biomolecular targets such as peptides, mucleotides, phospholipids, and carbohydrates are anionic compounds.[4a] Some polyaza macrocyclic ligands and cryptands, which incorporate two polyamine binding subunits located at the two poles of the structure, have been shown to recognize various anions through CH··· and NH··· anion interactions.[3] The bis-tren cryptands such as L, L^1, and L^2 (Scheme 1) can incorporate two metal ions at the two poles, leaving two axial sites vacant and favorable for the coordination of an anion.[4] Fabbrizzi et al.[4c] found that a dicopper(II) complex with the flexible L^2 can bind to halide anions. This flexible

Scheme 1

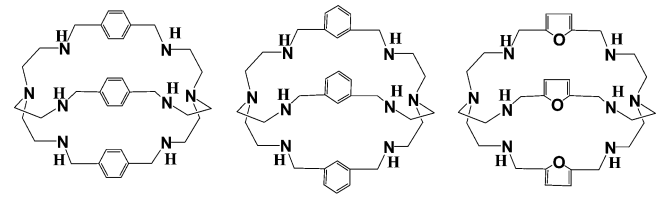

L L^1 L^2

* To whom correspondence should be addressed. E-mail: lutongbu@mail.sysu.edu.cn. Phone: +86-20-84112921. Fax: +86-20-84112921.

(1) Lehn, J.-M. *Angew. Chem., Int. Ed. Engl.* **1988**, *27*, 89.
(2) (a) Davis, A. P. *Coord. Chem. Rev.* **2006**, *250*, 2939. (b) Garcia-Espana, E.; Diaz, P.; Llinares, J. M.; Bianchi, A. *Coord. Chem. Rev.* **2006**, *250*, 2952. (c) Katayev, E. A.; Ustynyuk, Y. A.; Sessler, J. L. *Coord. Chem. Rev.* **2006**, *250*, 3004. (d) Schmuck, C. *Coord. Chem. Rev.* **2006**, *250*, 3053. (e) Gunnlaugsson, T.; Glynn, M.; Tocci, H. G.; Kruger, P. E.; Pfeffer, F. M. *Coord. Chem. Rev.* **2006**, *250*, 3094. (f) Rice, C. R. *Coord. Chem. Rev.* **2006**, *250*, 3190.
(3) (a) Gale, P. A.; Quesada, R. *Coord. Chem. Rev.* **2006**, *250*, 3219. (b) Kang, S. O.; Hossain, A. M.; Bowman-James, K. *Coord. Chem. Rev.* **2006**, *250*, 3038. (c) Wichmann, K.; Antonioli, B.; Sohnel, T.; Wenzel, M.; Gloe, K.; Price, J. R.; Lindoy, L. F.; Blake, A. J.; Schroder, M. *Coord. Chem. Rev.* **2006**, *250*, 2987. (d) Garcı´a-España, E.; Dı´az, P.; Llinares, J. M.; Bianchi, A. *Coord. Chem. Rev.* **2006**, *250*, 2952. (e) Kruppa, M.; König, B *Chem. Rev* **2006**, *106*, 3520. (f) Bowman-James, K. *Acc. Chem. Res.* **2005**, *38*, 671. (g) Hossain, M. A.; Morehouse, P.; Powell, D.; Bowman-James, K. *Inorg. Chem.* **2005**, *44*, 2143. (h) Mckee, V.; Nelson, J.; Town, R. M. *Chem. Soc. Rev.* **2003**, *32*, 309.
(4) (a) O'Neil, E. J.; Smith, B. D. *Coord. Chem. Rev.* **2006**, *250*, 3068. (b) Amendola, V.; Bonizzoni, M.; Esteban-Gomez, D.; Fabbrizzi, L.; Licchelli, M.; Sancenon, F.; Taglietti, A. *Coord. Chem. Rev.* **2006**, *250*, 1451. (c) Amendola, V.; Bastianello, E.; Fabbrizzi, L.; Mangano, C.; Pallavicini, P.; Perotti, A.; Lanfredi, A. M.; Ugozzoli, F. *Angew. Chem., Int. Ed.* **2000**, *39*, 2917. (d) Lu, Q.; Latour, J.-M.; Harding, C. J.; Martin, N.; Marrs, D. J.; McKee, V.; Nelson, J. *J. Chem. Soc., Dalton Trans.* **1994**, 1471. (e) Fabbrizzi, L.; Leone, A.; Taglietti, A. *Angew. Chem., Int. Ed.* **2001**, *40*, 3066. (f) Boiocchi, M.; Bonizzoni, M.; Fabbrizzi, L.; Piovani, G.; Taglietti, A. *Angew. Chem., Int. Ed.* **2004**, *43*, 3847. (g) Zhuang, X. M.; Lu, T. B.; Chen, S. *Inorg. Chim. Acta* **2005**, *358*, 2129. (h) Ravikumar, I.; Suresh, E.; Ghosh, P. *Inorg. Chem.* **2006**, *45*, 10046.

10.1021/ic702143d CCC: $40.75
Published on Web 03/05/2008

cryptate can contract and expand its Cu···Cu separation to include other anions from shorter OH^- to longer N_3^- and NCS^-.[4c,d] However, the flexible cryptate is not favorable for anion recognition because it has poor selectivity for a particular anion. The recognition of these dinuclear cryptates to anions depends on the flexibility and rigidity of the cryptands, as well as the M···M separations in the cryptates. Increasing the rigidity of a cryptate may improve its selectivity, as the M···M distance can be fixed within a narrow range for a rigid cryptate; thus, it can recognize an anion with particular size and shape.

Continuing our efforts on the recognition and activation of small guest molecules by cryptates,[5] we found that the rigid $[Co_2L]^{4+}$ can recognize Cl^- and Br^- but not F^- and I^-. Herein we report the structures of $[Co_2L(Cl)](ClO_4)_3$ (**1**), $[Co_2L(Br)](ClO_4)_3$ (**2**), and $[Co_2L(OH)(OH_2)]I_3$ (**3**), as well as the binding constants of $[Co_2L]^{4+}$ to Cl^- and Br^-. For comparison, the structure of $[Co_2L^1(Cl)](ClO_4)_3$ (**4**), in which L^1 is moderately rigid between L and L^2, and the binding constant of $[Co_2L^1]^{4+}$ to Cl^- are also presented. On the basis of the results of X-ray diffraction analysis, density functional theory (DFT) calculations, and the binding constants, it can be found that $[Co_2L]^{4+}$, in which L has a relative rigid tripodal skeleton, shows higher affinity toward Cl^- because of the size matching.

Experimental Section

Materials and Methods. The ligand L was prepared by a literature method, [6] L^1 was prepared by a modified literature method.[5b] All the other solvents and chemicals are commercially available and used without further purification. Elemental analyses were obtained using Elementar Vario EL elemental analyzer. The IR spectra were recorded in the 4000–400 cm^{-1} region at room temperature by using KBr pellets and a Bruker EQUINOX 55 spectrometer. UV–vis spectra were determined on a Shimadzu UV-3150 spectrophotometer. Magnetic susceptibility data for **1** and **2** were collected in the 2–300 K temperature range with a quantum design SQUID magnetometer MPMS XL-7 and a field of 0.1 T. A correction was made for the diamagnetic contribution prior to data analysis.

Caution! *Perchlorate salts of metal complexes with organic ligands are potentially explosive and should be handled with great care.*

$[Co_2L(Cl)](ClO_4)_3$ (1). A solution of $L\cdot 0.5H_2O$ (243 mg, 0.40 mmol) in methanol/acetonitrile (1:1, 10 mL) was added dropwise to a solution of $Co(ClO_4)_2\cdot 6H_2O$ (292 mg, 0.80 mmol) and NH_4Cl (22 mg, 0.40 mmol) in methanol/acetonitrile (1:1, 10 mL) or (n-$Bu)_4NCl$ (112 mg, 0.40 mmol) in acetonitrile (10 mL). The mixture was stirred at room temperature for 4 h. The purple precipitate obtained was filtered off, washed with ethanol, and then dissolved in a large amount of acetonitrile. The resulting solution was evaporated slowly at room temperature to give dark purple crystals of $1\cdot 2H_2O\cdot 3CH_3CN$ (348 mg, 72%). Anal. Calcd for $C_{38}H_{63}N_9Co_2Cl_4O_{14}$, ($1\cdot 2H_2O\cdot CH_3CN$): C, 40.40; H, 5.62; N, 11.16. Found: C, 39.96; H, 5.59; N, 11.39%. IR (KBr): 3430 (m), 3268 (w), 2882 (w), 1631 (w), 1519 (m), 1441 (m), 1111 (s), 1090 (s), 813 (m), 626 (m) cm^{-1}.

$[Co_2L(Br)](ClO_4)_3$ (2). This compound was prepared as dark purple crystals of $2\cdot 2H_2O\cdot 3CH_3CN$ in 69% yield, by a similar procedure to **1** from the reaction of $Co(ClO_4)_2\cdot 6H_2O$, $L\cdot 0.5H_2O$, and (n-$Bu)_4NBr$. Anal. Calcd for $C_{36}H_{54}N_8Co_2BrCl_3O_{12}$ (**2**): C, 39.49; H, 4.97; N, 10.23. Found: C, 39.78; H, 5.22; N, 10.13%. IR (KBr): 3436 (s), 3139 (s), 2916 (m), 2865 (m), 1654 (m), 1442 (s), 1072 (s), 1018 (s), 806 (s), 424 (m) cm^{-1}.

$[Co_2L(OH)(OH_2)]I_3$ (3). A solution of $L\cdot 0.5H_2O$ (243 mg, 0.40 mmol) in methanol/acetonitrile (1:1, 10 mL) was added dropwise to a solution of $Co(ClO_4)_2\cdot 6H_2O$ (292 mg, 0.80 mmol) and KI (266 mg, 1.60 mmol) in acetonitrile (10 mL). The mixture was stirred at room temperature for 4 h. The green precipitate obtained was filtered off, washed with ethanol, and dried in vacuum. Green crystals of $3\cdot H_2O$ were obtained by diffusion of ethyl acetate into the DMF solution of the solid (331 mg, 57%). Anal. Calcd for $C_{36}H_{59}N_8Co_2I_3O_3$ ($3\cdot H_2O$): C, 37.58; H, 5.17; N, 9.74. Found: C, 37.08; H, 5.34; N, 9.88%. IR (KBr): 3426 (s), 3267 (m), 2931 (w), 2882 (w), 1636 (w), 1520 (w), 1442 (m), 1114 (s), 1091 (s), 812 (m), 627 (m) cm^{-1}.

$[Co_2L^1(Cl)](ClO_4)_3$ (4). This compound was prepared as purple crystals of $4\cdot H_2O\cdot CH_3CN$ in 62% yield, by a similar procedure to **1** from the reaction of $Co(ClO_4)_2\cdot 6H_2O$, L^1, and (n-$Bu)_4NCl$. Anal. Calcd for $C_{36}H_{56}N_8Co_2Cl_4O_{13}$ ($4\cdot H_2O$): C, 40.46; H, 5.28; N, 10.48. Found: C, 39.85; H, 5.21; N 10.46%. IR (KBr): 3432 (s), 3265 (s), 2931 (m), 2881 (m), 1638 (w), 1578 (w), 1440 (m), 1115 (s), 1020 (s), 810 (m), 626 (s) cm^{-1}.

Crystal Structure Analyses. Single-crystal data for $1\cdot 2H_2O\cdot 3CH_3CN$, $2\cdot 2H_2O\cdot 3CH_3CN$, **3**, and $4\cdot H_2O\cdot CH_3CN$ were collected on a Bruker Smart 1000 CCD diffractometer with Mo Kα radiation ($\lambda = 0.71073$ Å). All empirical absorption corrections were applied by using the SADABS program.[7] The structures were solved using a direct method, which yielded the positions of all nonhydrogen atoms. These were refined first isotropically and then anisotropically to convergence. Though the axial OH^- and H_2O in **3** are crystallographically equivalent, the position is disordered, and the free variable refinement shows that the occupancy of two positions (O(1) and O(1′)) are approximately equal (6:4), with different Co−O distances. All the hydrogen atoms (except those bound to water molecules) were placed in calculated positions with fixed isotropic thermal parameters and included in the structure factor calculations in the final stage of the full-matrix least-squares refinement. All calculations were performed using the SHELXTL-97 system of computer programs.[8] Details of data collection, structure solution, and refinements can be found in Table 1. Relevant bond lengths and angles are included in Table 2.

Computational Details. The DFT calculations and geometry optimizations were performed with the Gaussian 03 package[9] based on the structural cations of **1**, **2**, and **4**, using the functional UB3LYP,[10] LANL2DZ basis set along with the corresponding pseudopotentials for cobalt, chloride, and bromide, and the 6–31G(d) basis set for all the other atoms. For reasons of computational expense due to the large size of our systems, frequency calculations have not been carried out on the minima. The graphical representations of the orbitals were produced by the gOpenMol[11] graphics program. The optimized Cartesian coordinates are given in the Supporting Information Table S1. The selected bond distances for optimized geometries are summarized in the Supporting Information Table S2. The Milliken and natural electron charges on cobalt, Cl^-/

(5) (a) Lu, T. B.; Zhuang, X. M.; Li, Y. W.; Chen, S. *J. Am. Chem. Soc.* **2004**, *126*, 4760. (b) Chen, J. M.; Wei, W.; Feng, X. L.; Lu, T. B. *Chem. Asian J.* **2007**, *2*, 710.
(6) Chen, D.; Martell, A. E. *Tetrahedron* **1991**, *47*, 6895.
(7) Sheldrick, G. M. *SADABS: Program for Empirical Absorption Correction of Area Detector Data*; University of Göttingen: Göttingen, Germany, 1996.
(8) Sheldrick, G. M. *SHELXTL-97: Program for Crystal Structure Solution and Refinement*; University of Göttingen: Göttingen, Germany, 1997.

Table 1. Crystallographic Data for **1**−**4**

compound	**1**·2H$_2$O·3CH$_3$CN	**2**·2H$_2$O·3CH$_3$CN	**3**	**4**·H$_2$O·CH$_3$CN
empirical formula	$C_{42}H_{67}Cl_4Co_2N_{11}O_{14}$	$C_{42}H_{67}BrCl_3Co_2N_{11}O_{14}$	$C_{36}H_{57}Co_2I_3N_8O_2$	$C_{38}H_{59}Co_2Cl_4N_9O_{13}$
fw	1209.73	1254.19	1132.46	1109.6
temp (K)	293	293	293	293
cryst syst	triclinic	triclinic	orthorombic	monoclinic
space group	$P\bar{1}$	$P\bar{1}$	*Pnnm*	$P2_1/c$
a (Å)	13.0784(14)	13.2069(14)	14.965(2)	14.3681(13)
b (Å)	13.9894(15)	14.0364(15)	15.044(2)	18.475(3)
c (Å)	15.6486(17)	15.7383(17)	27.198(4)	24.750(3)
α (°)	87.556(2)	87.381(2)	90	90
β (°)	66.632(2)	66.139(2)	90	95.289(3)
γ (°)	81.950(2)	82.061(2)	90	90
V (Å^3)	2602.1(5)	2642.4(5)	6123.2(15)	4720.6(11)
Z	2	2	4	4
ρ_{calcd} (g·cm^{-3})	1.544	1.574	1.248	1.561
μ (mm^{-1})	0.917	1.608	2.085	1
reflns collected	14218	19250	29229	26162
unique reflns. (R_{int})	10432 (0.0262)	10267 (0.0216)	6089 (0.0737)	9244 (0.0529)
S on F^2	1.049	1.021	1.028	1.012
R_1,[a] wR_2[b] ($I > 2\sigma(I)$)	0.0733, 0.1685	0.0424, 0.1058	0.0629, 0.1709	0.0482, 0.1077
R_1,[a] wR_2[b] (all data)	0.1081, 0.1875	0.0752, 0.1247	0.1416, 0.2174	0.1179, 0.1520

[a] $R_1 = \Sigma\, F_o| - |F_c|/\Sigma F_o$. [b] $wR_2 = [\Sigma[w(F_o^2 - F_c^2)^2]/\Sigma w(F_o^2)^2]^{1/2}$, where $w = 1/[\sigma^2(F_o)^2 + (aP)^2 + bP]$ and $P = (F_o^2 + 2F_c^2)/3$.

Br^- bridge, and phenyl rings are listed in the Supporting Information Table S3.

Results and Discussion

X-Ray Structures. The X-ray crystallographic analyses reveal that **1** and **2** are isomorphous, both crystallizing in space group $P\bar{1}$ (see Table 1). As shown in Figure 1a, the tripodal skeleton of L forces the Co(II) ions to adopt a five-coordinated geometry instead of a six-coordinated one. Each Co(II) ion is coordinated with four amine nitrogen atoms of L and one bridged Cl^- or Br^- anion. The parameters (τ) for the geometries[12] of the five-coordinated Co(II) ions are 1.02 and 1.03 for the two Co(II) ions in **1** and 1.01 and 1.03 in **2**, where $\tau = 1.00$ for TBP (trigonal bipyramidal) and 0.00 for SP (square pyramidal), indicating that the geometries of Co(II) in both cryptates are ideal TBPs. In both cryptates, the two bridgehead nitrogen atoms, the two Co(II) ions, and the Cl^-/Br^- anion are almost collinear. The Co−Cl distances are slightly shorter than the Co−Br distances while the Co−N (bridgehead) distances in **1** are slightly longer than those in **2** (see Table 2). In both cryptates, the Co−N (bridgehead) distances (2.247(3)−2.272(4) Å) are longer than the other Co−N distances (2.113(4)−2.130(4) Å). The Co···Co separation in **1** (4.866(3) Å) is shorter than that in **2** (5.034(3) Å). The Cl···centroid (see Figure 1a) distances are 3.246, 3.221, and 3.219 Å, respectively, and the Br···centroid distances are 3.266, 3.243, and 3.239 Å, respectively. These distances are shorter than the sum of the van der Waals radii of Cl···C (3.45 Å) and Br···C (3.55 Å), demonstrating the existence of interactions between the Cl^-/Br^- and the phenyl rings of L in **1** and **2**. As shown in Figure 1b,c, the rigid triangle conformation of L makes the Cl^-/Br^- tightly encapsulated in the cryptate, resulting in a well wrapped stable cryptate. The average Cl···centroid distance is only about 0.02 Å smaller than the average Br···centroid distance, though Br^- is 0.15 Å larger than Cl^-, indicating that the Br^- is more squeezed within the three triangle shaped phenyl rings of L. Hence, $[Co_2L(Br)]^{3+}$ may be less stable than $[Co_2L(Cl)]^{3+}$ because of unfavorable Br···π distances.

The structure of **4** is similar to that of **1**, in which each Co(II) ion is five-coordinated with four amine nitrogen atoms of L[1] and one bridged Cl^- anion (Figure 2a), and the geometries of Co(II) are also TBPs ($\tau = 1.02$ for Co1 and 1.03 for Co2). The two bridgehead nitrogen atoms, the two Co(II) ions, and the Cl^- anion are almost collinear. The distance between the two bridgehead nitrogen atoms (9.186 Å) is shorter than that in **1** (9.446 Å), and the Co−Cl and Co−N (bridgehead) distances, as well as the Co···Co separation in **4**, are all shorter than those in **1** (see Table 2). The Cl···centroid (see Figure 2a) distances are 3.370, 3.322 to 3.300 Å, respectively. The average Cl···centroid distance in **4** is about 0.1 Å longer than that in **1**. The position of chloride in **4** is off center (Figure 2b), the angles of the Cl···centroid axis to the planes of the phenyl rings are 72, 74, and 76°, respectively, while the chloride in **1** locates the

(9) Frisch, M. J.; Trucks, G. W.; Schlegel, H. B.; Scuseria, G. E.; Robb, M. A.; Cheeseman, J. R.; Montgomery, J. A.; Vreven, T., Jr.; Kudin, K. N.; Burant, J. C.; Millam, J. M.; Iyengar, S. S.; Tomasi, J.; Barone, V.; Mennucci, B.; Cossi, M.; Scalmani, G.; Rega, N.; Petersson, G. A.; Nakatsuji, H.; Hada, M.; Ehara, M.; Toyota, K.; Fukuda, R.; Hasegawa, J.; Ishida, M.; Nakajima, T.; Honda, Y.; Kitao, O.; Nakai, H.; Klene, M.; Li, X.; Knox, J. E.; Hratchian, H. P.; Cross, J. B.; Adamo, C.; Jaramillo, J.; Gomperts, R.; Stratmann, R. E.; Yazyev, O.; Austin, A. J.; Cammi, R.; Pomelli, C.; Ochterski, J. W.; Ayala, P. Y.; Morokuma, K.; Voth, G. A.; Salvador, P.; Dannenberg, J. J.; Zakrzewski, V. G.; Dapprich, S.; Daniels, A. D.; Strain, M. C.; Farkas, O.; Malick, D. K.; Rabuck, A. D.; Raghavachari, K.; Foresman, J. B.; Ortiz, J. V.; Cui, Q.; Baboul, A. G.; Clifford, S.; Cioslowski, J.; Stefanov, B. B.; Liu, G.; Liashenko, A.; Piskorz, P.; Komaromi, I.; Martin, R. L.; Fox, D. J.; Keith, T.; Al-Laham, M. A.; Peng, C. Y.; Nanayakkara, A.; Challacombe, M.; Gill, P. M. W.; Johnson, B.; Chen, W.; Wong, M. W.; Gonzalez, C.; Pople, J. A., *Gaussian 03*, revision C.02; Gaussian, Inc.: Pittsburgh, PA, 2003.

(10) Casellas, H.; Massera, C.; Buda, F.; Gamez, P.; Reedijk, J. *New J. Chem.* **2006**, *30*, 1561.

(11) (a) Laaksonen, L. *J. Mol. Graphics* **1992**, *10*, 33. ; a graphics program for the analysis and display of molecular dynamics trajectories. (b) Bergman, D. L.; Laaksonen, L.; Laaksonen, A. *J. Mol. Graphics. Modell.* **1997**, *15*, 301. ; visualization of solvation structures in liquid mixtures.

(12) Addison, A. W.; Rao, T. N.; Reedijk, J.; van Rijn, J.; Verschoor, G. C. *J. Chem. Soc., Dalton Trans.* **1984**, 1349.

Table 2. Selected Bond Distances (Å) and Angles (°) for **1**–**4**

		Compound **1**	
Co(1)−Cl(1)	2.4359(13)	Co(2)−Cl(1)	2.4303(13)
Co(1)−N(1)	2.269(4)	Co(2)−N(5)	2.272(4)
Co(1)−N(2)	2.130(4)	Co(2)−N(6)	2.126(4)
Co(1)−N(3)	2.124(4)	Co(2)−N(7)	2.116(4)
Co(1)−N(4)	2.118(4)	Co(2)−N(8)	2.113(4)
N(4)−Co(1)−N(3)	116.16(15)	N(4)−Co(1)−N(2)	116.83(16)
N(3)−Co(1)−N(2)	117.16(15)	N(4)−Co(1)−N(1)	79.37(15)
N(3)−Co(1)−N(1)	79.71(15)	N(2)−Co(1)−N(1)	79.23(14)
N(4)−Co(1)−Cl(1)	101.01(12)	N(3)−Co(1)−Cl(1)	100.77(11)
N(2)−Co(1)−Cl(1)	99.92(10)	N(1)−Co(1)−Cl(1)	179.15(11)
N(8)−Co(2)−N(7)	116.14(16)	N(8)−Co(2)−N(6)	116.53(15)
N(7)−Co(2)−N(6)	117.50(15)	N(8)−Co(2)−N(5)	79.89(15)
N(7)−Co(2)−N(5)	79.21(16)	N(6)−Co(2)−N(5)	79.26(15)
N(8)−Co(2)−Cl(1)	99.44(11)	N(7)−Co(2)−Cl(1)	102.03(11)
N(6)−Co(2)−Cl(1)	100.17(11)	N(5)−Co(2)−Cl(1)	178.76(12)
Co(2)−Cl(1)−Co(1)	179.15(6)		
		Compound **2**	
Co(1)−Br(1)	2.5148(6)	Co(2)−Br(1)	2.5191(6)
Co(1)−N(1)	2.248(3)	Co(2)−N(5)	2.247(3)
Co(1)−N(2)	2.130(3)	Co(2)−N(6)	2.131(3)
Co(1)−N(3)	2.115(3)	Co(2)−N(7)	2.115(3)
Co(1)−N(4)	2.115(3)	Co(2)−N(8)	2.120(3)
N(7)−Co(2)−N(8)	116.95(12)	N(7)−Co(2)−N(6)	117.15(12)
N(8)−Co(2)−N(6)	117.64(12)	N(7)−Co(2)−N(5)	80.36(12)
N(8)−Co(2)−N(5)	80.47(11)	N(6)−Co(2)−N(5)	80.21(11)
N(7)−Co(2)−Br(1)	99.82(9)	N(8)−Co(2)−Br(1)	99.93(8)
N(6)−Co(2)−Br(1)	99.21(8)	N(5)−Co(2)−Br(1)	179.41(8)
N(3)−Co(1)−N(4)	116.87(12)	N(3)−Co(1)−N(2)	118.17(12)
N(4)−Co(1)−N(2)	117.09(12)	N(3)−Co(1)−N(1)	80.30(12)
N(4)−Co(1)−N(1)	80.79(11)	N(2)−Co(1)−N(1)	80.66(11)
N(3)−Co(1)−Br(1)	100.89(8)	N(4)−Co(1)−Br(1)	98.63(8)
N(2)−Co(1)−Br(1)	98.73(8)	N(1)−Co(1)−Br(1)	178.81(8)
Co(1)−Br(1)−Co(2)	178.94(2)		
		Compound **3**	
Co(1)−O(1)	2.019(5)	Co(1)-O(1′)	1.822(5)
Co(1)−N(1)	2.240(6)	Co(1)−N(2)	2.179(7)
Co(1)−N(3)	2.180(7)	Co(1)−N(4)	2.156(5)
O(1′)-Co(1)−N(4)	100.3(2)	O(1)−Co(1)−N(4)	101.5(2)
O(1′)-Co(1)−N(2)	97.7(2)	O(1)−Co(1)−N(2)	101.8(2)
N(4)−Co(1)−N(2)	114.4(2)	O(1′)-Co(1)−N(3)	103.8(2)
O(1)−Co(1)−N(3)	98.6(2)	N(4)−Co(1)−N(3)	115.7(2)
N(2)−Co(1)−N(3)	1120.0(3)	O(1′)-Co(1)−N(1)	176.2(3)
O(1)−Co(1)−N(1)	178.2(2)	N(4)−Co(1)−N(1)	79.6(2)
N(2)−Co(1)−N(1)	78.9(2)	N(3)−Co(1)−N(1)	79.6(2)
		Compound **4**	
Co(1)−Cl(4)	2.3617(11)	Co(2)−Cl(4)	2.3713(11)
Co(1)−N(5)	2.229(3)	Co(2)−N(1)	2.224(3)
Co(1)−N(6)	2.117(3)	Co(2)−N(2)	2.126(3)
Co(1)−N(7)	2.110(3)	Co(2)−N(3)	2.091(3)
Co(1)−N(8)	2.117(3)	Co(2)−N(4)	2.104(3)
N(7)−Co(1)−N(8)	117.45(13)	N(7)−Co(1)−N(6)	116.98(13)
N(8)−Co(1)−N(6)	117.91(13)	N(7)−Co(1)−N(5)	80.86(12)
N(8)−Co(1)−N(5)	80.48(12)	N(6)−Co(1)−N(5)	80.81(12)
N(7)−Co(1)−Cl(4)	99.32(10)	N(8)−Co(1)−Cl(4)	99.58(9)
N(6)−Co(1)−Cl(4)	98.94(9)	N(5)−Co(1)−Cl(4)	179.75(9)
N(3)−Co(2)−N(4)	117.80(13)	N(3)−Co(2)−N(2)	117.16(13)
N(4)−Co(2)−N(2)	117.79(13)	N(3)−Co(2)−N(1)	81.17(13)
N(4)−Co(2)−N(1)	80.71(12)	N(2)−Co(2)−N(1)	81.03(12)
N(3)−Co(2)−Cl(4)	98.18(9)	N(4)−Co(2)−Cl(4)	100.26(9)
N(2)−Co(2)−Cl(4)	98.64(10)	N(1)−Co(2)−Cl(4)	179.02(10)
Co(1)−Cl(1)−Co(2)	178.75(5)		

center of each phenyl ring, with the angles of 90° (Figure 1b). The longer Cl···centroid distances and the off-center position of Cl^- in **4** indicate that the stability of $[Co_2L^1]^{4+}$ toward Cl^- is less than that of $[Co_2L]^{4+}$ toward Cl^- because of the relatively flexible structure of L^1.

In contrast to **1** and **2**, the I^- anions in **3** are not encapsulated in the cavity of the cryptate but located outside as counteranions. The axial positions of two five-coordinated Co(II) ions are occupied by one OH^- and one water molecule, respectively (Figure 3). The parameter (τ) for the geometry[12] of the five-coordinated Co(II) ion is 0.97, indicating the geometries of the two Co(II) in **3** are also

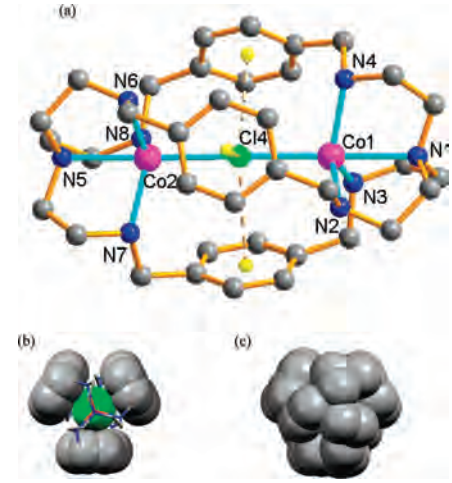

Figure 1. (a) Structure, (b) triangle geometry, and (c) space-filling representation of $[Co_2L(Cl)]^{3+}$ in **1**, indicating Cl^- is well encapsulated inside the cavity of the cryptate. The $[Co_2L(Br)]^{3+}$ in **2** is isomorphous.

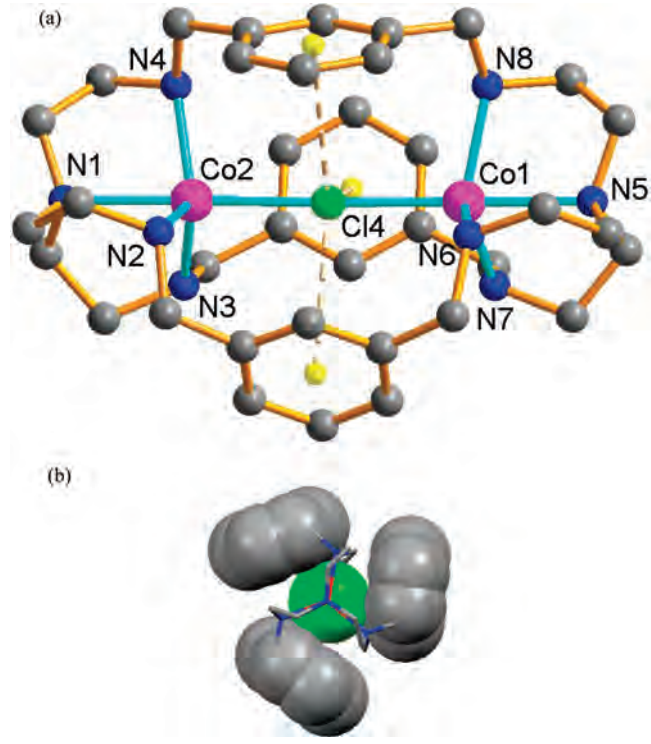

Figure 2. (a) Structure and (b) triangle geometry of $[Co_2L^1(Cl)]^{3+}$ in **4**.

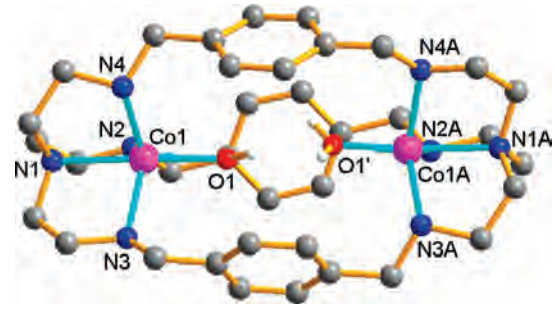

Figure 3. Structure of $[Co_2L(OH)(OH_2)]^{3+}$ in **3**.

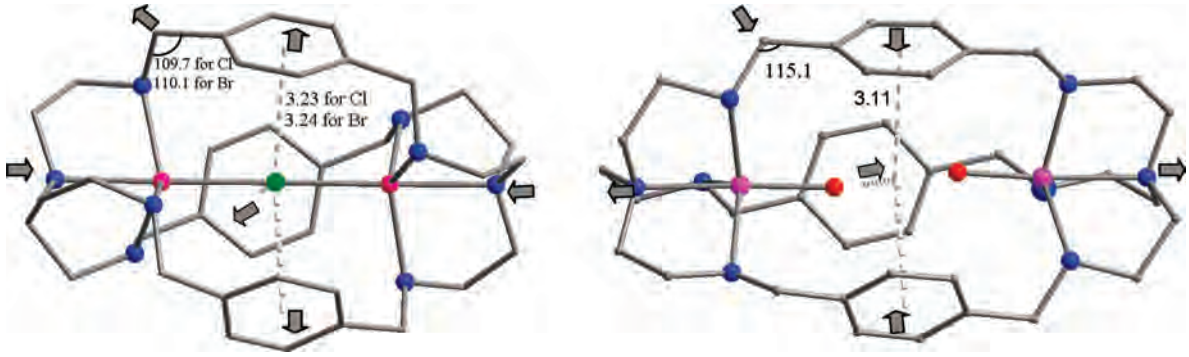

Figure 4. Structures of **1, 2** (left), and **3** (right), showing that reducing or extending the Co···Co separation will extend (left) or contract (right) the centroid (axial)···centroid (phenyl) distance, respectively.

TBPs. The Co−N (bridgehead) distance (2.240(6) Å) is longer than the other Co−N distances ((2.155(5)−2.182(7) Å). The O(1)···O(1′) separation of 2.665(6) Å (the O(1)···O(1A) and O(1′)···O(1′A) separations are 2.454(6) Å) is much longer than that of 2.325(9) Å in $[Cu_2L(OH)(OH_2)]^{3+}$.[13] The extremely shorter O···O separation in the latter is asserted to be squeezed by the cryptate encapsulation,[13] and this is not true based on the structure of **3** because the Co···Co separation can be expanded to 6.482(2) Å in **3**. A recent report also indicates that the Cu···Cu separation in $[Cu_2L(N_3)]^{3+}$ can be expanded to 6.188 Å.[4h] These separations are all longer than the Cu···Cu separation in $[Cu_2L(OH)(OH_2)]^{3+}$ (6.121(1) Å).[13]

It is interesting to note that $[Co_2L]^{4+}$ can encapsulate Cl^- and Br^- but not I^-. As shown in Figure 4, **1** and **2** show close Cl/Br···centroid distances (3.23 Å for Cl^- and 3.24 Å for Br^-, average distances) and N−C−C angles (109.7 for Cl^- and 110.1° for Br^-, average). In **3**, the longer Co···Co separation results in the larger N−C−C angle (115.1°, average) and shorter centroid (axial)···centroid (phenyl) distance (3.11 Å, average). These indicate that the extension of the Co···Co separation will shorten the centroid (axial)···centroid (phenyl) distance. However, encapsulation of the larger I^- anion by $[Co_2L]^{4+}$ needs to significantly expand the Co···Co separation and the centroid (axial)···centroid (phenyl) distances simultaneously, and this is impossible to achieve in the rigid $[Co_2L]^{4+}$. Therefore, I^- can not be encapsulated inside the cavity of $[Co_2L]^{4+}$. It is not surprising that the F^- bridged compound also cannot be formed because its too small radius and the rigid structure of L.

DFT Calculations. Further insight into the halide encapsulated electronic structures is obtained by the DFT calculations based on the structural cations of **1**, **2**, and **4**. The DFT-BLYP geometry optimizations for all the halide encapsulated structures show that a local minimum exists in good agreement with the corresponding X-ray structures (Supporting Information Table S2). This agreement is representative for the employed level of theory. Details of the charge distribution diagram and the frontier molecular orbital diagram of the optimized structures are given in Figure 5 and Supporting Information Figures S1−S3. The Milliken and natural net electron charges (Supporting Information Table S3) of the halide is less negative than −1, indicating a very significant donation from the halide to the d orbitals of Co(II) upon coordination. Meanwhile, the Milliken and natural net electron charges of each phenyl ring is positive, indicating that phenyl ring is electron-deficient due to the connection with the $-CH_2-N-Co$ group. All of these enhance the electron-poor character of both the halide ions and the phenyl rings, make them less repulsed, and thus result in a well wrapped stable cryptate. For all the halide encapsulated structures, there are four binding molecular orbitals, α-HOMO-8, α-HOMO-9, β-HOMO-6, and β-HOMO-7, between phenyl rings and Cl^-/Br^- anions, suggesting the interactions between phenyl rings and Cl^-/Br^- may exist in **1**, **2,** and **4**.

UV–vis Spectra. Compounds **1** and **2** display similar electronic spectra, which are different from that of **3** (Figure 6). The purple solutions of **1** and **2** in acetonitrile show the values of absorbance at 528 (ε = 138 L·mol^{-1}·cm^{-1}), 612 (ε = 169 L·mol^{-1}·cm^{-1}), and 880 (ε = 30 L·mol^{-1}·cm^{-1}) nm for **1**, and 538 (ε = 125 L·mol^{-1}·cm^{-1}), 616 (ε = 215 L·mol^{-1}·cm^{-1}), and 858 (ε = 32 L·mol^{-1}·cm^{-1}) nm for **2**. The green solution of **3** in acetonitrile shows two absorption bands at 456 and 643 nm. The absorption band of **1** at 612 nm, which is absent in **3**, with a lower intensity than that of **2** at 616 nm, can be attributed to an $X^- \rightarrow$ Co(II) charge-transfer transition.[14]

A green solution appeared when an acetonitrile solution of L was added to an acetonitrile solution containing two equivalents of $Co(ClO_4)_2 \cdot 6H_2O$. Adding Cl^- or Br^- to this green solution caused an immediate color change from green to purple, demonstrating that a Cl^- or Br^- bridged cryptate was formed in solution. However, the green color persisted after adding Cl^- or Br^- to an acetonitrile solution of **3**. This implies that the initially formed green cryptate in acetonitrile is $[Co_2L]^{4+}$ instead of $[Co_2L(OH)]^{3+}$, in which the axial position is thought to be "void" or, more realistically, occupied by water or acetonitrile molecules[4c] which are easy to replace with Cl^- or Br^-. This result is in agreement with that of ESI-MS measurement (Supporting Information Figure

(13) Bond, A. D.; Derossi, S.; Jensen, F.; Larsen, F. B.; McKenzie, C. J.; Nelson, J. *Inorg. Chem.* **2005**, *44*, 5987.

(14) (a) Ciampolini, M.; Nardi, N. *Inorg. Chem.* **1967**, *6*, 445. (b) Ciampolini, M.; Paoletti, P. *Inorg. Chem.* **1967**, *6*, 1261. (c) Zinn, P. J.; Powell, D. R.; Day, V. W.; Hendrich, M. P.; Sorrell, T. N.; Borovik, A. S. *Inorg. Chem.* **2006**, *45*, 3484.

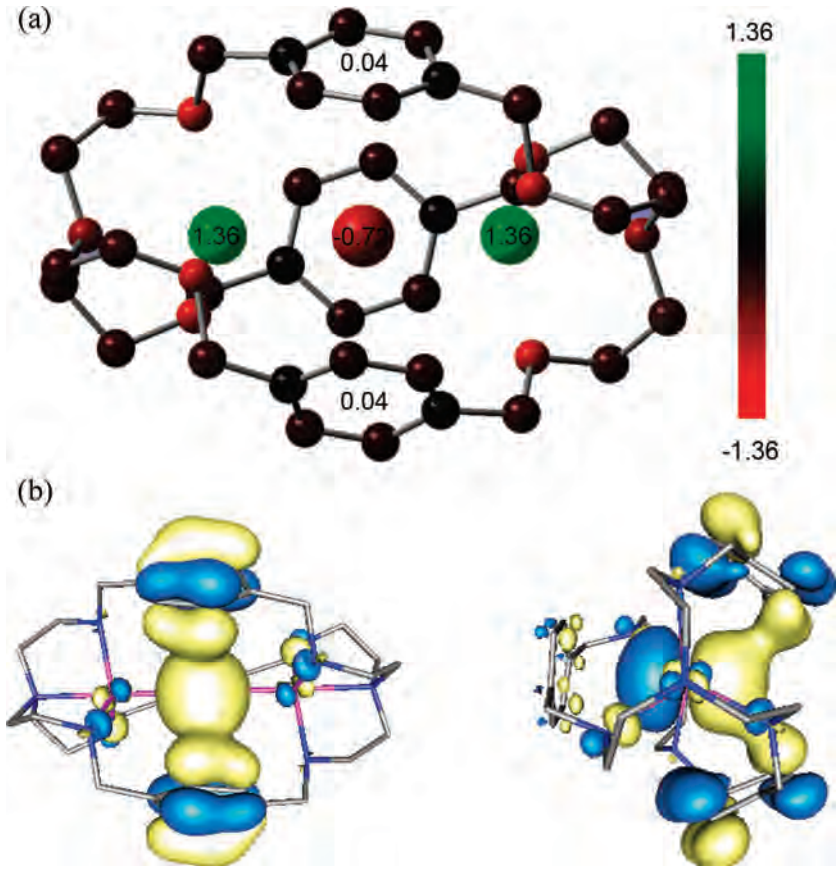

Figure 5. (a) Natural net electron charge distribution diagram, and (b) the binding molecular orbital α-HOMO-8 between phenyl rings and Br^- in $[Co_2L(Br)]^{3+}$ (left) and a view along the Co_2 axis (right).

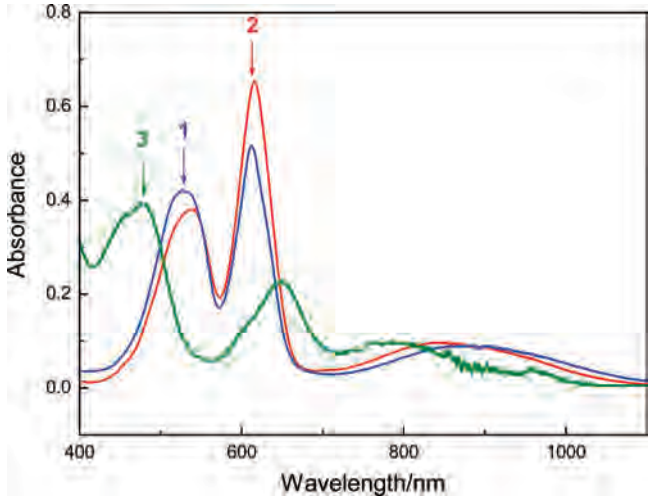

Figure 6. UV–vis spectra of **1**, **2,** and **3** in acetonitrile.

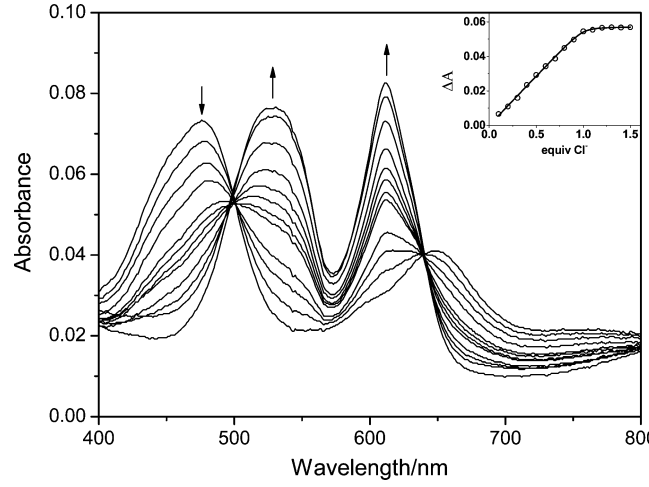

Figure 7. Titration of an acetonitrile solution of $[Co_2L]^{4+}$ (6.0×10^{-4} mol·L^{-1}) with Cl^-. The growing bands at 530 and 612 nm correspond to the formation of $[Co_2L(Cl)]^{3+}$. The inset shows a curve-fitting plot of the spectra titration at 612 nm, indicating that a 1:1 inclusion compound is formed.

S8a), in which only species corresponding to $[Co_2L]^{4+}$ and $[CoL]^{2+}$ appeared in solution.

The binding property of $[Co_2L]^{4+}$ toward halides was investigated by the UV–vis spectra. The Job's plot of $[Co_2L]^{4+}$ with Cl^- at 612 nm (and Br^- at 616 nm) in acetonitrile displays a maximum absorbance value at $0.5 = [Cl^-]/\{[Cl^-] + [Co_2L]^{4+}\}$ (and $0.5 = [Br^-]/\{[Br^-] + [Co_2L]^{4+}\}$, indicating that a 1:1 inclusion compound is formed (Supporting Information Figure S4). To quantify the binding constants of $[Co_2L]^{4+}$ toward Cl^- and Br^- anions, an acetonitrile solution containing L (6.0×10^{-4} mol·L^{-1} for Cl^- and 4.0×10^{-4} mol·L^{-1} for Br^-) and two equivalents of $Co(ClO_4)_2 \cdot 6H_2O$ was titrated with a standard solution of $(n\text{-Bu})_4NCl$ or $(n\text{-Bu})_4NBr$ in acetonitrile. A typical family of spectra recorded during the titration with Cl^- is shown in Figure 7. From Figure 7 it can be found that the initial peaks around 475 and 650 nm disappeared, and two new peaks at 530 and 612 nm appeared, along with adding of Cl^-, indicating that Cl^- bridged cryptate is formed in solution

upon adding of Cl^-. The titration profile corresponding to the formation of a 1:1 inclusion compound is shown in Figure 7. The binding constants for the equilibrium $[Co_2L]^{4+} + Cl^- \leftrightarrow [Co_2L(Cl)]^{3+}$ can be obtained using the following equation:[15]

$$\Delta A = \frac{\Delta\varepsilon([H]_0 + [G]_0 + \frac{1}{K_S}) \pm \sqrt{\Delta\varepsilon([H]_0 + [G]_0 + \frac{1}{K_S})^2 - 4\Delta\varepsilon^2[H]_0[G]_0}}{2} \quad (1)$$

where ΔA and $\Delta\varepsilon$ denote the changes in the absorbance (at 612 nm) and in the molar extinction coefficient of $[Co_2L(Cl)]^{3+}$ and $[Co_2L]^{4+}$, respectively, and $[H]_0$ and $[G]_0$ represent the initial concentrations of $[Co_2L]^{4+}$ and Cl^-, respectively. A nonlinear least-squares fitting of all experimental points leads to a log K value of 5.7(1). Absorption titrations were repeated at a different concentration of $[Co_2L]^{4+}$ (8×10^{-4} mol·L^{-1}) and gave a close log K value of 5.69(9). An analogous titration profile for Br^- was obtained with a log K value of 5.2(1) (Supporting Information Figure S5). The smaller log K value for Br^- is due to the weaker crystal field strength of Br^-[16] and its larger ion radius, as the cavity of the cryptate is too crowded for Br^- at the radial position for the rigid structure of $[Co_2L]^{4+}$.

Similar to **1**, the purple solutions of **4** in acetonitrile show three absorption bands at 520 ($\varepsilon = 186$ L·mol^{-1}·cm^{-1}), 611 ($\varepsilon = 221$ L·mol^{-1}·cm^{-1}), and 810 ($\varepsilon = 48$ L·mol^{-1}·cm^{-1}) nm (Supporting Information Figure S6). The Job's plot of $[Co_2L^1]^{4+}$ with Cl^- at 611 nm in acetonitrile also indicates a 1:1 inclusion compound is formed (Supporting Information Figure S4). The titration of $[Co_2L^1]^{4+}$ with Cl^- gave a log K value of 4.2(1) (Supporting Information Figure S5), which is 1.7 units less than that of $[Co_2L]^{4+}$ with Cl^-, indicating that the relatively more rigid tripodal skeleton of L than that of L^1 results in the higher affinity of $[Co_2L]^{4+}$ toward Cl^-. This demonstrates that increasing the rigidity of a cryptate can indeed improve its selectivity toward a halide.

When $(n\text{-Bu})_4NF$ or $(n\text{-Bu})_4NI$ was added to an acetonitrile solution of $[Co_2L]^{4+}$, the green color of the solution persisted, and the positions of two bands at 475 and 650 nm were shifted to 460 and 640 nm and to 475 and 633 nm before and after adding F^- or I^-, respectively (Figure 8). The Job's plots of $[Co_2L]^{4+}$ with F^- at 460 nm and with I^- at 633 nm in acetonitrile do not show maximum absorbance values at $0.5 = [F^-/I^-]/\{[F^-/I^-] + [Co_2L]^{4+}\}$ (Supporting Information Figure S7). In addition, the ESI-MS measurements indicate that adding equivalents of $(n\text{-Bu})_4NF$ to a solution of $[Co_2L]^{4+}$ in acetonitrile did not afford peaks corresponding to $[Co_2L(F)]^{3+}$ and $[Co_2L(F_2)]^{2+}$ species (Supporting Information Figure S8). These clearly demonstrate that 1:1 (for F^- and I^-) or 1:2 (for F^-) inclusion compounds were not formed in solution. Moreover, the precipitate appeared in solution when excess

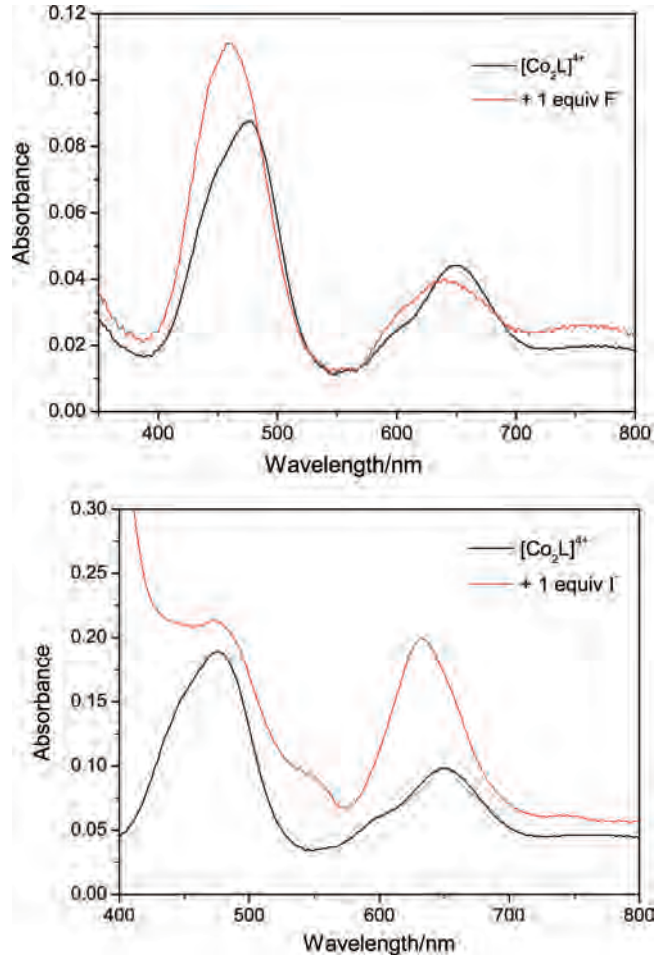

Figure 8. UV–vis spectra of adding equivalents of F^- (top) and I^- (bottom) to a solution of $[Co_2L]^{4+}$ in acetonitrile.

of F^- was added to an acetonitrile solution of $[Co_2L]^{4+}$ (it began to precipitate when the molar ratio of $F^-/[Co_2L]^{4+}$ is over 1 in 1.6×10^{-3} mol·L^{-1} of $[Co_2L]^{4+}$), indicating that insoluble N−H···F^-···H−N linked polymer probably is formed in solution because of the strong N−H···F^- hydrogen bonding interactions (if F^- encapsulated complex is formed, it should be soluble in acetonitrile). Indeed, there are intermolecular N−H···I^-···H−N hydrogen bonding interactions in the crystal structure of **3** (Supporting Information Figure S9). Therefore, the peak shifts and absorbance intensity increase after adding F^- and I^- to $[Co_2L]^{4+}$ (Figure 8) may be attributed to the intermolecular N−H···F^-/I^-···H−N hydrogen bonding interactions, which increase the electric density of coordinated nitrogen atoms of L, and thus increase the intensity of the d−d transitions of the Co(II) ions. The I^- can donate more electrons to the coordinated nitrogen atoms through the N−H···I^- hydrogen bonding interactions; thus, the intensity of the absorbance increased more when I^- was added. In addition, when four equivalents of I^- was added to an acetonitrile solution of $[Co_2L]^{4+}$, the absorption bands at 475 and 633 nm disappeared, and new bands corresponding to $[CoI_4]^{2-}$ appeared[16a] (Supporting Information Figure S10), indicating that the transformation from $[Co_2L]^{4+}$ to

(15) Liu, Y.; Han, B. H.; Zhang, H. Y. *Curr. Org. Chem.* **2004**, *8*, 35.
(16) (a) Cotton, F. A.; Goodgame, D. M. L.; Goodgame, M. *J. Am. Chem. Soc.* **1961**, *83*, 4690. (b) Fine, D. A. *J. Am. Chem. Soc.* **1962**, *84*, 1139.

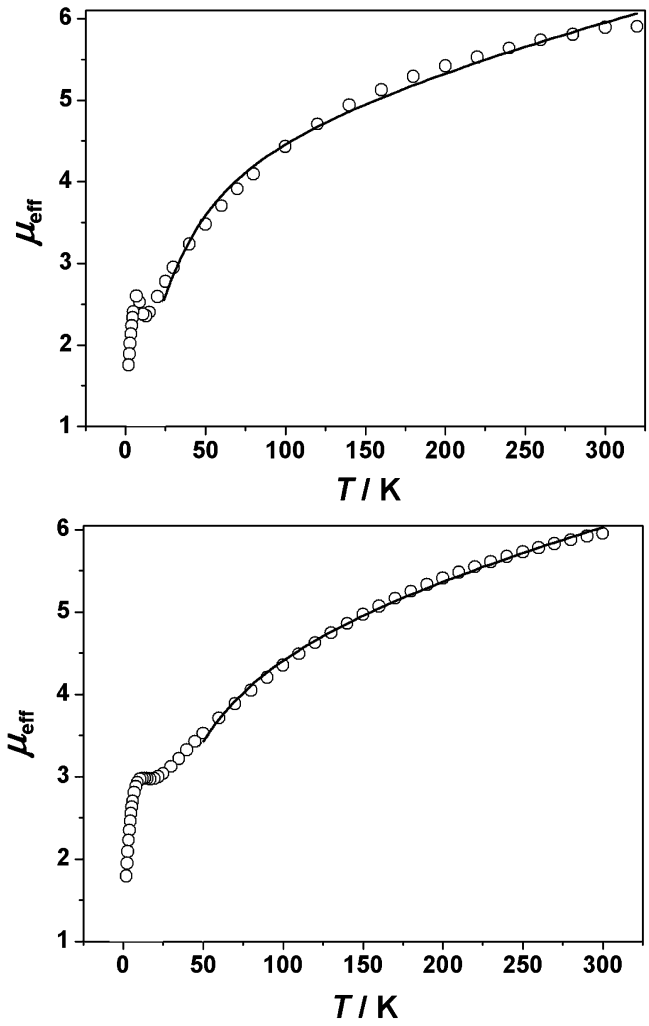

Figure 9. Temperature dependences of μ_{eff} for **1** (top) and **2** (bottom). The solid lines are the best-fit curves.

$[CoI_4]^{2-}$ had occurred. The ESI-MS measurement also indicates the formation of the $[CoI_3(ClO_4)]^{2-}$ (m/z = 539.8) species in solution.

Magnetic Properties. The temperature dependencies of μ_{eff} for **1** and **2** are shown in Figure 9. The μ_{eff} values at room temperature, 5.90 μ_B for **1** and 5.95 μ_B for **2**, are larger than the expected value of 5.48 μ_B for two uncoupled Co(II) ions ($S = 3/2$, $g = 2.0$). The μ_{eff} values gradually decrease along with decreasing temperature to minimum values of 1.75 μ_B for **1** and 1.79 μ_B for **2** at 2.0 K. This behavior is typical of an antiferromagnetic coupling, indicating Cl^- and Br^- bridged cryptates were formed. The experimental magnetic data were analyzed using the isotropic spin Hamiltonian $H = -JS_1 \cdot S_2$. The magnetic equation is as follows:[17]

$$\chi_A = \frac{Ng^2\beta^2}{kT}\frac{e^x + 5e^{3x} + 14e^{6x}}{1 + 3e^x + 5e^{3x} + 7e^{6x}} + N\alpha \qquad (2)$$

where $\chi = J/(kT)$, and the other symbols have their usual meanings. The refinement gave the fit parameters with g = 2.19(10), $J = -13.7(14)$ cm^{-1}, $N\alpha = 7.9(8) \times 10^{-3}$ cm^{-1} for **1** and $g = 2.22(6)$, $J = -17.1(12)$ cm^{-1}, $N\alpha = 8.3(4) \times 10^{-3}$ cm^{-1} for **2**. The larger J value for Br^- is in agreement with the trend observed in other halide bridged compounds, in which the magnetic coupling through the halide bridge increases along with decreasing electronegativity of the halide.[18]

Conclusions

The present study demonstrates that a rigid dicobalt(II) cryptate $[Co_2L]^{4+}$ can recognize Cl^- and Br^- but not F^- and I^-. To our knowledge, this is the first example in which a cryptate displays selective binding to part of the halide ions and does not bind to the rest of the halide ions at all. The special affinity of $[Co_2L]^{4+}$ toward Cl^- is attributable to the size matching to the rigid cavity of $[Co_2L]^{4+}$. As we expect, increasing the rigidity of a cryptate can improve its selectivity to anions. Thus, $[Co_2L]^{4+}$ can be used as an efficient colorimetric sensor for Cl^- and Br^-. At present, we are investigating the selectivity of $[Co_2L^1]^{4+}$ toward halides and the recognition of $[Co_2L]^{4+}$ to other polyatomic anions.

Acknowledgment. This work was supported by NSFC (20625103), NSF of Guangdong Province (04205405), and 973 Program of China (2007CB815305).

Supporting Information Available: X-ray crystallographic files in CIF format, the correlative theory calculation results, and UV–vis spectra of the interactions of the cryptates with halides (PDF). This material is available free of charge via the Internet at http://pubs.acs.org.

IC702143D

(17) (a) Kahn, O. *Mol. Magn.* **1993**, 114. (b) Hossain, M. J.; Sakiyama, H. *Inorg. Chim. Acta* **2002**, *338*, 255.
(18) (a) Lever, A. B. P.; Thompson, L. K.; Reiff, W. M. *Inorg. Chem.* **1972**, *11*, 104. (b) Mealli, C.; Midollini, S.; Sacconi, L. *Inorg. Chem.* **1975**, *14*, 2513.